Sādhanā (2020)45:106
https://doi.org/10.1007/s12046-020-01355-9

Grey-fuzzy method-based parametric analysis of abrasive water jet machining on GFRP composites

VIDYAPATI KUMAR[1], PARTHA PROTIM DAS[2] and SHANKAR CHAKRABORTY[3,*]

[1]Central Institute of Mining and Fuel Research, Dhanbad, Jharkhand, India
[2]Department of Mechanical Engineering, Sikkim Manipal Institute of Technology, Sikkim Manipal University, Majitar, Sikkim, India
[3]Department of Production Engineering, Jadavpur University, Kolkata, West Bengal, India
e-mail: crewvidyapati@gmail.com; parthaprotimdas@ymail.com; s_chakraborty00@yahoo.co.in

MS received 6 November 2019; revised 14 March 2020; accepted 16 March 2020

Abstract. Abrasive water jet machining (AWJM) is an advanced non-traditional material removal process which can machine almost all types of thin hard-to-cut materials. The quality of its machining operation can be effectively enhanced while selecting the appropriate settings of its different input parameters through the application of optimization techniques. This paper aims in obtaining the optimal combination of four AWJM control parameters, such as water jet pressure, stand-off distance, abrasive mass flow rate and traverse speed while machining of glass fiber reinforced polymer (GFRP) composites. Grey relational analysis combined with fuzzy logic is employed here for attaining the most favored values of the process outputs (responses), i.e. material removal rate, surface roughness, kerf width and kerf angle. The effects of varying AWJM process parameters on the measured responses are further studied through the developed interaction plots, while the contributions of those process parameters are identified through analysis of variance technique. The response surface plots would further help in determining the attainable values of the corresponding process parameters to realize the desired quality of the considered responses.

Keywords. AWJM process; GFRP; grey theory; fuzzy logic; process parameter; response.

1. Introduction

Abrasive water jet machining (AWJM) is an advanced non-traditional machining process, being extensively employed in many industrial and manufacturing applications. It basically combines the material removal mechanisms of water jet machining (WJM) and abrasive jet machining (AJM) processes. It is a cold machining process in which abrasives are proportionately mixed with an extremely fine jet of water travelling at high velocity ($\approx$ 1000 m/s) to aid the material removal operation from hard materials by plastic deformation, erosion and fracture of the workpiece [1]. The kinetic energy of the water jet increases with its velocity. While performing cutting operation using smaller diameter jets, although the mass flow rate is decreased, the kinetic energy of the jet increases with increased velocity imparted by high pressure ($\approx$ 200 to 400 MPa). When this pressurized water jet is directed to the work material to be cut, its velocity becomes virtually zero after striking the workpiece surface and almost all of its possessed kinetic energy is transformed into pressure energy [2]. Some portion of the impulsive force of water is also transferred as kinetic energy to the abrasive particles, thereby rapidly increasing their velocity to help in material removal. This process has several advantages, like high machining performance, low cutting force, no residual stress formation, high flexibility, eco-friendliness, no heat affected zone, ability to generate complex shapes, etc. [3, 4]. In this process, as the tool never comes in direct contact with the workpiece, the mechanical characteristics of the work material are almost retained. These advantageous features of AWJM process make it suitable for machining of stainless steel, titanium, aluminum, Inconel, brass, granite, glass, coal, plastics, composites, etc. which have found wide ranging applications in automotive, nuclear, aerospace, oil, medical and construction industries [5–7]. Nowadays, it has also been effectively utilized in the manufacturing industries as a suitable substitute for wire electrical discharge machining, plasma arc machining and laser cutting processes [8]. Generation of intense noise and an untidy machining environment are its major disadvantages. The AWJM process can cut metallic plates up to 10 mm thickness *while maintaining the desired dimensional accuracy. For thick components, the cutting rate would gradually decrease which would be responsible for taper and waviness of the machined components. It is also

*For correspondence
Published online: 06 May 2020

an expensive process, unsuitable for mass production because of its high maintenance requirements [2]. The cutting capability of this process is determined by several factors, like early degradability of the work material, reactivity of the work material with water and abrasives, hardness of the work material, etc.

Simply, an AWJM set-up comprises a water pump, an abrasive water jet nozzle, an abrasive feed system and a catcher. By means of a high pressure water pump, the pumping system delivers water at a very high velocity that increases the pressure with respect to a specific mass flow rate of water. Besides being a carrier for the abrasives, the water also serves as a cooling medium and flushes off the eroded workpiece materials from the cutting zone. It also prevents the abrasives from spreading away after exit from the nozzle. During the cutting operation, the stand-off distance is so chosen that the passage gap becomes very small not allowing the abrasives to disperse. Abrasives are mixed with high velocity water through a controlled nozzle where kinetic energy of the water jet is transmitted to the abrasive particles. These abrasives are blended with water in two ways, i.e. (a) they are supplied through the conical-shaped nozzle to the water flowing through its center, and (b) water is directly supplied to the centrally jetted abrasive particles. After the machining operation, high velocity water is collected in a catcher, which is placed just underneath the workpiece. The workpiece is positioned on a grid directly above the catcher so that the entire energy of the pressurized water jet can be effectively utilized during the machining operation.

It has been observed that various AWJM control parameters, like water jet pressure, abrasive mass flow rate, stand-off distance, traverse speed, impact angle of the jet, abrasive grit size, etc. play significant roles in achieving the desired machining performance of this process with respect to material removal rate (MRR), surface roughness (SR), kerf width (KW), kerf angle (KA), etc. Thus, the study of various AWJM process parameters along with their effects on the process outputs (responses) is supposed to be extremely crucial to investigate the stochastic material removal mechanism of this process. It also demands identification of the optimal parametric mix of different process parameters for attaining improved machining condition for AWJM process.

2. Review of literature

This section presents a review of the current literature available on parametric study of AWJM processes. Based on Taguchi's experimental design plan, Jegaraj and Babu [9] investigated the effects of orifice and variation in focusing tube bore on depth of cut, KW and SR while AWJ cutting of aluminum 6063-T6 alloy. Azmir and Ahsan [10] observed that nature of the abrasive material, hydraulic pressure, stand-off distance and traverse rate had significant influence on SR of glass fiber reinforced epoxy composite materials. Srinivasu and Babu [11] developed a neuro-genetic model to determine the settings of various AWJ cutting parameters, like water jet pressure, abrasive flow rate and jet traverse rate for attaining the desired value of depth of cut. The depth of cut was also predicted based on an artificial neural network (ANN) model. Applying Taguchi method and response surface methodology (RSM), Siddiqui *et al*. [12] examined the influences of water jet pressure, abrasive flow rate and quality level on SR while performing AWJ cutting operation on Kevlar composite materials. Zain *et al.* [13] combined ANN with simulated annealing (SA) technique to identify the best parametric settings of water jet pressure, stand-off distance, abrasive flow rate, abrasive grit size and traverse speed to achieve the minimum value of SR during AWJM operation. Zain *et al.* [14] presented the simultaneous application of genetic algorithm (GA) and SA techniques to search out the optimal parametric mix for achieving better performance of an AWJM process. Pawar and Rao [15] adopted teaching-learning-based optimization (TLBO) algorithm for finding out the best parametric condition of an AWJM process. Its effectiveness was also contrasted with that of other popular optimization techniques. Kartal *et al.* [16] studied the influences of abrasive flow rate, nozzle feed rate and spindle speed on MRR and SR while performing AWJ turning operation on low density polyethylene materials. In an AWJ turning operation, Liu *et al.* [17] applied RSM technique along with desirability function approach to examine the influences of different input parameters on depth of penetration and SR of the machined components. Mellal *et al.* [18] proposed the applications of cuckoo search (CS) algorithm and hoopoe heuristic for optimization of various input parameters of an AWJM process. Aich *et al.* [19] employed SA and particle swarm optimization (PSO) algorithms for attaining better performance of an AWJM process with respect to MRR and depth of cut while machining borosilicate glass materials. Using Taguchi method-based grey relational analysis (GRA), Munuswamy and Krishnan [20] determined the optimal combinations of water jet pressure, traverse speed and stand-off distance for having minimum values of SR and KA while performing AWJM operation on aluminum alloy AA 6351 material.

Naresh Babu and Muthukrishnan [21] considered abrasive flow rate, stand-off distance, feed rate and water pressure as the input parameters of an AWJM process, and identified their optimal conditions for having minimum SR value based on the application of desirability function approach. Using GRA technique, Singh and Chaturvedi [22] determined the best parametric combination of stand-off distance, water pressure, abrasive flow rate and traverse speed to achieve the maximum MRR and minimum SR values. Yuvaraj and Pradeep Kumar [23] employed technique for order of preference by similarity to ideal solution (TOPSIS) as a multi-response optimization tool for

Table 1. Optimization techniques applied in AWJM processes.

Sl. No.	Authors	Process parameters	Response(s)	Optimization technique(s) applied
1.	Srinivasu and Babu [11]	Water pressure, jet traverse rate, abrasive flow rate	Depth of cut	Hybrid ANN, GA
2.	Siddiqui *et al*. [12]	Water pressure, quality level, abrasive flow rate	SR	Taguchi method, RSM
3.	Zain *et al*. [13]	Water pressure, traverse speed, abrasive grit size, abrasive flow rate, stand-off distance	SR	ANN, SA
4.	Zain *et al*. [14]	Water pressure, traverse speed, abrasive grit size, abrasive flow rate, stand-off distance	SR	GA, SA
5.	Kartal *et al*. [16]	Abrasive flow rate, spindle speed, nozzle feed rate	SR, MRR	Taguchi method
6.	Liu *et al*. [17]	Traverse speed, pressure, tilt angle, surface speed, stand-off distance, abrasive flow rate	Depth of penetration, SR	RSM with desirability function
7.	Aich *et al*. [19]	Traverse speed, abrasive flow rate, water pressure, stand-off distance	MRR, depth of cut	SA, PSO
8.	Munuswamy and Krishnan [20]	Traverse speed, stand-off distance, water jet pressure	MRR, KA	Taguchi-GRA
9.	Naresh Babu and Muthukrishnan [21]	Water pressure, feed rate, abrasive flow rate, stand-off distance	SR	RSM with desirability function
10.	Singh and Chaturvedi [22]	Abrasive flow rate, traverse speed, water pressure, stand-off distance	MRR, SR	GRA
11.	Yuvaraj and Kumar [23]	Water pressure, traverse rate, abrasive flow rate, stand-off distance	Depth of penetration, cutting rate, SR, taper cut ratio, top KW	TOPSIS
12.	Chaturvedi and Singh [24]	Traverse speed, stand-off distance, abrasive flow rate, water pressure	MRR, SR	VIKOR
13.	Ghosh *et al*. [25]	Traverse speed, stand-off distance, water pressure, abrasive flow rate	SR, MRR, KW	Grey-Taguchi method
14.	Santhanakumar *et al*. [27]	Stand-off distance, abrasive flow rate, abrasive grain size, water pressure, traverse speed	SR, taper angle	Grey-Taguchi method

Table 1 continued

Sl. No.	Authors	Process parameters	Response(s)	Optimization technique(s) applied
15.	Nair and Kumanan [28]	Water pressure, table feed, abrasive flow volume, stand-off distance	MRR, parallelism, circularity, perpendicularity, cylindricity	WPCA
16.	Kumar *et al.* [30]	Abrasive flow rate, traverse speed, water pressure, stand-off distance	SR	RSM
17.	Chakraborty and Mitra [32]	Water pressure, abrasive concentration, jet velocity, nozzle diameter, nozzle tip distance	MRR, SR, overcut, taper	Grey wolf optimizer
18.	Kumar *et al.* [33]	Stand-off distance, traverse speed, percent content of tungsten carbide	MRR, SR	RSM
19.	Present paper	Water pressure, stand-off distance, abrasive flow rate, traverse speed	MRR, SR, KW, KA	Grey-fuzzy logic approach

attaining better realization of an AWJ cutting operation. While performing AWJM operation on stainless steel AISI 304 material, Chaturvedi and Singh [24] applied VIKOR (Vise kriterijumsko KOmpromisno Rangiranje) method to determine the most preferred settings of traverse speed, stand-off distance, abrasive flow rate and water pressure to achieve better MRR and SR values. Ghosh *et al.* [25] adopted grey-Taguchi method to identify the optimal settings of traverse speed, abrasive flow rate, stand-off distance and water pressure in an AWJ cutting process. In a hole-making operation on glass fiber reinforced polymer (GFRP) composites using AWJM process, Ibraheem *et al.* [26] examined the influences of water jet pressure, stand-off distance, fiber density, cutting speed and abrasive flow rate on the considered responses. Santhanakumar *et al.* [27] applied grey-Taguchi methodology to search out the best operating levels of stand-off distance, abrasive flow rate, abrasive grain size, water pressure and traverse speed for achieving the desired values of SR and taper angle of the machined components. Considering abrasive flow volume, water pressure, table feed rate and stand-off distance as the input parameters of an AWJM process, Nair and Kumanan [28] employed weighted principal component analysis (WPCA) as a multi-performance optimization tool for the said process. For an AWJM process, Shukla and Singh [29] compared the optimization performance of seven advanced evolutionary algorithms and concluded that biogeography-based algorithm would outperform the others with respect to the observed response values. Using the Box-Behnken experimental design plan, Kumar *et al.* [30] conducted experiments to analyze the influences of traverse speed, abrasive flow rate, stand-off distance and water pressure on SR of the machined components. Based on RSM technique, Babu and Muthukrishnan [31] developed the related regression equations showing the relationships of stand-off distance, water pressure, abrasive flow rate and feed rate with SR and KA in an AWJM process. Chakraborty and Mitra [32] employed grey wolf optimizer to identify the best combination of various input parameters in an AWJM process. The adopted mathematical tool could be applied for single and multi-objective optimization of the said process. With the purpose of optimizing MRR and SR in an AWJM process, Kumar *et al.* [33] determined the most favorable settings of stand-off distance, traverse speed and percent content of tungsten carbide using RSM-based models.

In table 1, an exhaustive list of the AWJM process parameters, responses and optimization techniques adopted by the past researchers is provided. Based on the observations from this table, it can be propounded that parametric optimization of AWJM process has drawn extensive attention of the researchers since several years. Various multi-criteria decision making tools, like TOPSIS, VIKOR, GRA, etc., and optimization methods, such as GA, SA, CS, PSO, and grey wolf optimizer. have been successfully deployed in order to derive the optimal parametric mixes

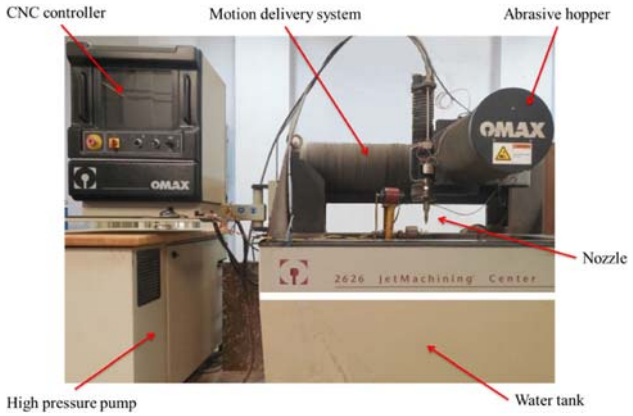

Figure 1. Photograph of the AWJM set-up.

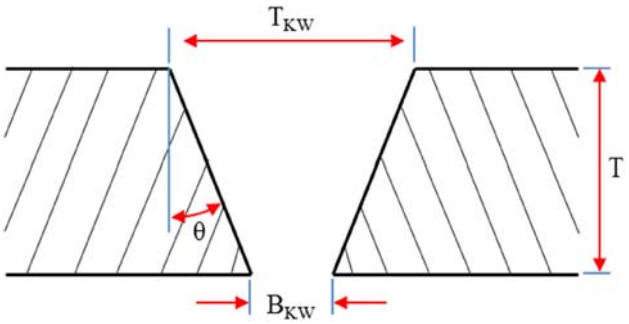

Figure 2. Measurement of kerf angle.

Table 2. AWJM process parameters with their levels.

Process parameter	Symbol	Unit	Level 1	Level 2	Level 3
Water jet pressure	A	MPa	165	215	265
Stand-off distance	B	mm	1	2	3
Abrasive mass flow rate	C	g/min	200	300	400
Traverse speed	D	mm/min	30	40	50

for enhanced operational performance of the AWJM processes. In this paper, a maiden attempt is put forward to experimentally examine the effects of various input parameters on different performance measures of an AWJM process through interaction plots during machining of GFRP composites. Additionally, the GRA method combined with fuzzy logic is employed to identify the optimal parametric mix for the said process. Application of grey-fuzzy approach for parametric optimization of AWJM process has not been reported in the literature till date. The analysis of variance (ANOVA) technique is also utilized to establish the contributions of the AWJM process parameters in determining the machining performance. Surface plots are finally developed to further help the process engineers in selecting the specific parametric mix to have the desired values of the considered responses.

3. Experimental results

The experiments have been conducted on an AWJM set-up (Make OMAX 2626), as shown in figure 1, which has a maximum pump capacity and operating pressure of 20 hp and 400 MPa respectively. As the workpiece material, GFRP composites have been chosen. Due to their several favorable mechanical properties, like high specific strength ($\approx$ 1324 MPa), high modulus of elasticity ($\approx$ 25 GPa), low weight (density $\approx$ 0.84 to 1.20 g/cc), low corrosion resistance ($\approx$ 3 to 4 in relative scale), etc., GFRP composites have now found wide ranging applications in oil, gas, aerospace and other process industries. They have been produced by hand lay-up process with bi-directional glass fiber material as the reinforcement and graphite powder as the filler material. The compositions of the graphite, glass fiber and epoxy in the samples have been around 3%, 50% and 47% respectively. The dimensions of the GFRP composites have been measured as 250 mm $\times$ 250 mm with a thickness of 8 mm. A straight through cut of 30 mm length has been made by the AWJM process. Four control parameters of the AWJM process, i.e. water jet pressure, stand-off distance, abrasive mass flow rate and traverse speed have been selected considering three level variations for each parameter, as exhibited in table 2. Other process parameters, like focusing length and impact angle have been kept constant at 0.76 mm and 90° respectively throughout the machining operation. Garnet with average mesh size 80 (i.e. 165 μm) has been taken as the abrasive particle. The diameter of the nozzle has been 0.70 mm and precision of the cutting head movement is $\pm$ 0.025 mm. Based on the literature survey, it has been observed that stand-off distance is one of the most significant technological factors influencing the quality characteristics of the machined components. A slight decrease in stand-off distance results in enhanced cutting accuracy with respect to reduced taper and SR due to better penetration capability. On the other hand, machining operation with low stand-off distance would generate a narrow cut on the workpiece surface restricting some of the abrasive particles to flow through which leads to their accumulation in the machining zone. Those abrasive particles would obstruct the new particles causing an increase in machining time. The experimental design has been planned based on Taguchi's L_9 orthogonal array while taking into account nine sets of experiments with various combinations of the considered process parameters. To study the machining effectiveness of the AWJM process on GFRP composites, four performance measures, i.e. MRR, SR, KW and KA have been selected as the responses.

Table 3. Experimental details.

Exp. No.	A	B	C	D	MRR (mm^3/min)	SR (μm)	KW (mm)	KA (degree)
1	165	1	200	30	252.0	1.53	1.05	0.5013
2	165	2	300	40	321.6	1.70	1.01	0.6087
3	165	3	400	50	362.0	1.73	0.91	0.1074
4	215	1	300	50	402.0	2.69	1.01	0.3223
5	215	2	400	30	252.0	2.13	1.05	0.3581
6	215	3	200	40	288.0	2.03	0.90	0.2865
7	265	1	400	40	316.8	2.68	0.99	0.4297
8	265	2	200	50	388.0	2.35	0.97	0.3581
9	265	3	300	30	255.6	3.98	1.07	0.5381

The value of MRR has been obtained as the quantity of workpiece material removed during unit machining time and can be calculated using Eq. (1). The SR value has been measured utilizing a surface roughness tester (Mitutoyo SJ-210), and has been the average of three test runs measured at the upper most, middle and lower most sides of the machined surface of GFRP composites. Kerf has been determined using an optical microscope having a magnification of 100X at three points each alongside the span of cut both on the top and bottom cut surfaces, known as top kerf width (T_{KW}) and bottom kerf width (B_{KW}) respectively. The KW has then been calculated by taking the average of T_{KW} and B_{KW}. The KA (θ) or kerf taper is an important quality characteristic of the machined components. Generally, a tapered slot of cut is generated during through cut operation of the work material where the KW at top is more than that at bottom. The tapered angle is the measure of angle of deviation between T_{KW} and B_{KW}, as shown in figure 2, and can be determined using Eq. (2).

$$MRR = KW \times TS \times T \tag{1}$$

$$\theta = \tan^{-1}\left(\frac{T_{KW} - B_{KW}}{2T}\right) \tag{2}$$

where T is the thickness of the GFRP composite.

The experimental plan along with the values of the measured responses for all the nine parametric combinations is provided in table 3. Among these responses, MRR is the lone response with larger-the-better quality characteristic. On the contrary, SR, KW and KA are of smaller-the-better quality characteristics.

4. Mathematical models

4.1 *Grey relational analysis*

The theory of grey system, first presented by Deng [34], implies the underprivileged, inadequate and indeterminate primitive data in a system, whereas, the grey relation defines the inadequate relation of information within the dataset. The GRA is the comparative analysis of the quantitative data among every data sequence, explaining the degree of correlation within the reference (ideal) sequence and an objective sequence (response values). The measured degree of correlation between these sequences is termed as grey relational coefficient (GRC). If the two considered sequences are of same importance (equal values), the corresponding GRC value becomes 1. In GRA technique, multi-response values can thus be transformed into a single grey relational grade (GRG), by taking the average of the GRC values of each sequence (response) for a corresponding alternative (experimental trial). An alternative is identified to be more important when its GRG value is found to be higher than the others.

In GRA technique, the initial stage belongs to the development of a decision matrix consisting of n criteria (responses) and m alternatives (experimental trials). The step-by-step procedure involved in GRA application is provided as below:

Step 1: Normalization of the decision matrix

The elements in the decision matrix are first normalized to bring them into a comparable range between 0 and 1, so as to remove variability and make the dataset dimensionless. In consideration to the type of quality characteristic, the following equations can be employed.

For larger-the-better type:

$$a_{ij}^{*} = \left(a_{ij} - \min a_{ij}\right) / \left(\max a_{ij} - \min a_{ij}\right),\ i = 1, 2, 3, \ldots, m;\ j = 1, 2, 3, \ldots, n \tag{3}$$

For smaller-the-better type:

$$a_{ij}^{*} = \left(\max a_{ij} - a_{ij}\right) / \left(\max a_{ij} - \min a_{ij}\right) \tag{4}$$

Where a_{ij} and a_{ij}^{*} are the measured and normalized values for i^{th} alternative with respect to j^{th} criterion.

Step 2: Computation of the GRC values

The GRC values are calculated from the normalized data for all the responses, using Eq. (5). They signify the

correlation between the best (ideal) and the obtained normalized values.

$$\xi_{ij} = (\delta_{\min} + \lambda\delta_{\max}) \Big/ \left(\delta_{ij}^{0} + \lambda\delta_{\max}\right) \tag{5}$$

where δ_{ij}^{0} is the variation between a_{ij}^{0} (ideal sequence) and a_{ij}^{*}. On the other hand, λ is the distinguishing coefficient, and it takes a value between 0 and 1, preferably 0.5. It is mostly responsible for expansion or compression of the range for GRC values. Furthermore, $\delta_{\min}$ and $\delta_{\max}$ are the global minima and global maxima values in different data series respectively. Larger value of GRC indicates an alternative to be nearer to the desired solution pertaining to a particular criterion.

Step 3: Calculation of the GRG values

The GRG values are now calculated while taking the arithmetic mean of the GRC values for each criterion related to each alternative.

$$G_i = \frac{1}{n}\sum_{j=1}^{n} \xi_{ij} \tag{6}$$

The alternative with the maximum GRG value is identified to be the best option signifying its dominance as compared to others for the said problem.

4.2 *Fuzzy rule-based modeling*

Fuzzy set theory [35] was mainly established to take into account the inaccurate information to have a reasonable agreement for a decision making problem. In this paper, GRA is coupled with fuzzy logic to overcome the uncertainties originated from considering larger-the-better and smaller-the-better types of quality characteristics. Fuzzy set theory makes use of various linguistic terms, like 'low', 'medium', 'high', etc. which are transformed into numeral values employing fuzzy membership functions. A fuzzy set involves a number of membership functions that map each and every element x into an universe of objects, say X to a real integer R within the range of [0,1]. The uncertainty involved in grey theory can thus be overcome while adopting fuzzy logic approach, thereby developing a fuzzy multi-performance tool, also known as grey-fuzzy logic approach.

A fuzzifier, fuzzy membership function, rule base, fuzzy inference engine and a defuzzifier are the primary components of a fuzzy logic approach. It mainly involves fuzzification of the input GRC values as linguistic terms through membership functions that map each input to a membership value from 0 to 1. Correspondingly, the inference engine accomplishes fuzzy inference based on the rule base to initiate a fuzzy value. The obtained fuzzy value is transformed into a crisp value, also known as grey-fuzzy reasoning grade (GFRG), using the defuzzifier. The fuzzy rule base mainly comprises a pool of 'If-then' rules generated to signify the inference correlation between the input GRC and output GFRG values. Typically, the set of rules can be represented as mentioned below:

1^{st} rule: If (a_1 is L_1) and (a_2 is M_1) and (a_3 is N_1) and (a_4 is O_1), then output (G is P_1).
2^{nd} rule: If (a_1 is L_2) and (a_2 is M_2) and (a_3 is N_2) and (a_4 is O_2), then output (G is P_2).
…
n^{th} rule: If (a_1 is L_n) and (a_2 is M_n) and (a_3 is N_n) and (a_4 is O_n), then output (G is P_n). (7)

where the fuzzy subsets L_i, M_i, N_i, O_i and P_i are defined by the concerned membership functions, i.e. μ_{Li}, μ_{Mi}, μ_{Ni}, μ_{Oi} and μ_{Pi} respectively. The fuzzy multi-response output, $\mu_{G_0}(G)$ can thus be calculated by means of max–min interface technique. The inferential outcome in a fuzzy system, comprising a number of membership functions for multiple responses, can be expressed as follows:

$$\begin{aligned}\mu_{G_0}(G) = {} & (\mu_{L_1}(a_1) \wedge \mu_{M_1}(a_2) \wedge \mu_{N_1}(a_3) \wedge \mu_{O_1}(a_4) \\ & \wedge \mu_{P_1}(G)) \vee (\mu_{L_2}(a_1) \wedge \mu_{M_2}(a_2) \wedge \mu_{N_2}(a_3) \\ & \wedge \mu_{O_2}(a_4) \wedge \mu_{P_2}(G)) \vee \ldots\ldots(\mu_{L_n}(a_1) \\ & \wedge \mu_{M_n}(a_2) \wedge \mu_{N_n}(a_3) \wedge \mu_{O_n}(a_4) \wedge \mu_{P_n}(G))\end{aligned} \tag{8}$$

where $\wedge$and $\vee$ are the minimum and maximum operations. At last, the generated fuzzy output can be defuzzified using various methods, like centroid fuzzification technique, weighted average technique, max–min membership technique, etc. The centroid fuzzification technique is mainly applied to convert the multi-response fuzzy output $(\mu_{G_0}(G))$ into the corresponding crisp value of GFRG, as it is a more predominant and substantial representation of all the methods.

$$GFRG = \frac{\sum G\mu_{G_0}(G)}{\sum \mu_{G_0}(G)} \tag{9}$$

The calculated GFRG values can then be organized in descending order, wherein the alternative with the largest value of GFRG is identified as the best option, while removing uncertainties and vagueness in the experimentally observed data. The GRA method coupled with fuzzy logic has been proved to be a simple and efficient approach in solving many complex multi-criteria problems dealing with determination of the optimal parametric combinations for diverse machining processes, like electrochemical machining [36], ultrasonic machining [36], light guide plate printing [37], bone drilling [38], ultrasonic-assisted electrical discharge machining [39], wire electrical discharge machining [40], thermal drilling [41], etc. This paper adopts grey-fuzzy approach as a multi-response optimization tool for determining the optimal settings of the considered AWJM process parameters.

Table 4. Normalized, GRC and GRG values.

	Normalized values of the experimental results				GRC				
Exp. No.	MRR	SR	KW	KA	MRR	SR	KW	KA	GRG
1	0	1	0.1176	0.2142	0.3333	1	0.3617	0.3889	0.5210
2	0.464	0.9306	0.3529	0	0.4826	0.8781	0.4359	0.3333	0.5325
3	0.7333	0.9184	0.9412	1	0.6522	0.8596	0.8947	1	0.8516
4	1	0.5265	0.3529	0.5713	1	0.5136	0.4359	0.5384	0.6220
5	0	0.7551	0.1176	0.4999	0.3333	0.6712	0.3617	0.5	0.4666
6	0.24	0.7959	1	0.6427	0.3968	0.7101	1	0.5832	0.6726
7	0.432	0.5306	0.4706	0.3571	0.4682	0.5158	0.4857	0.4375	0.4768
8	0.9067	0.6653	0.5882	0.4999	0.8427	0.599	0.5484	0.5	0.6225
9	0.024	0	0	0.1408	0.3388	0.3333	0.3333	0.3679	0.3433

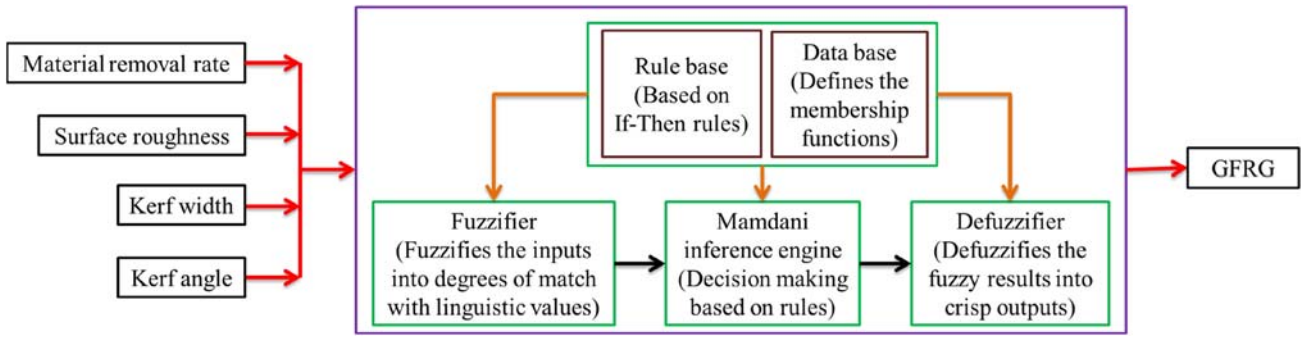

Figure 3. Grey-fuzzy model for the AWJM process.

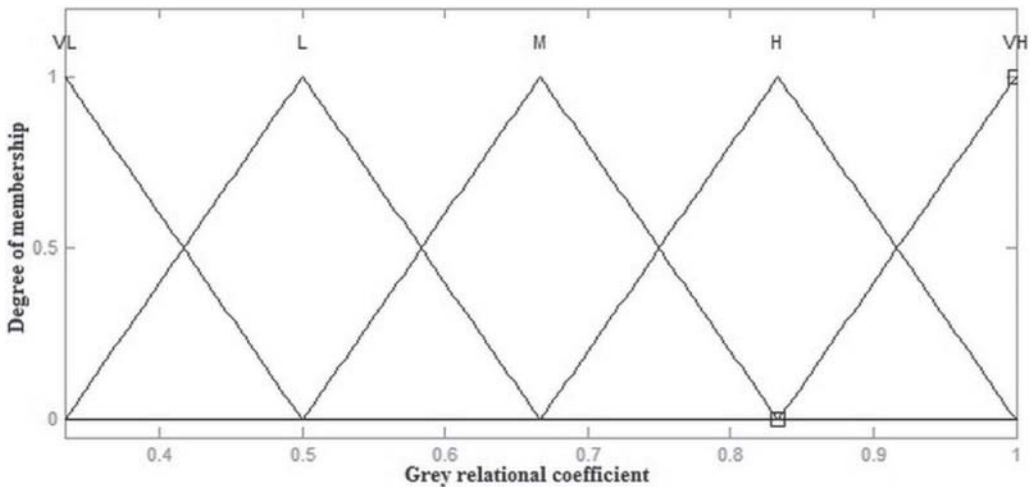

Figure 4. Input membership function.

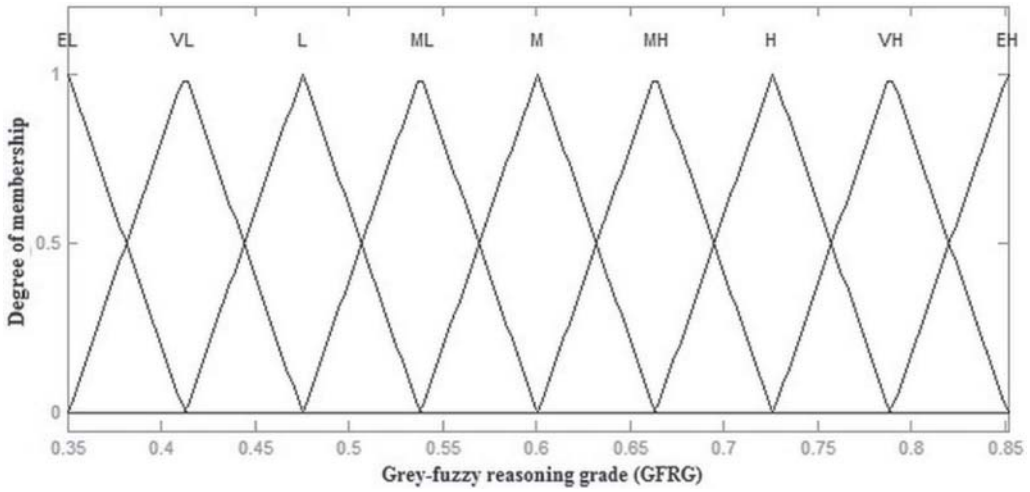

Figure 5. Output membership function.

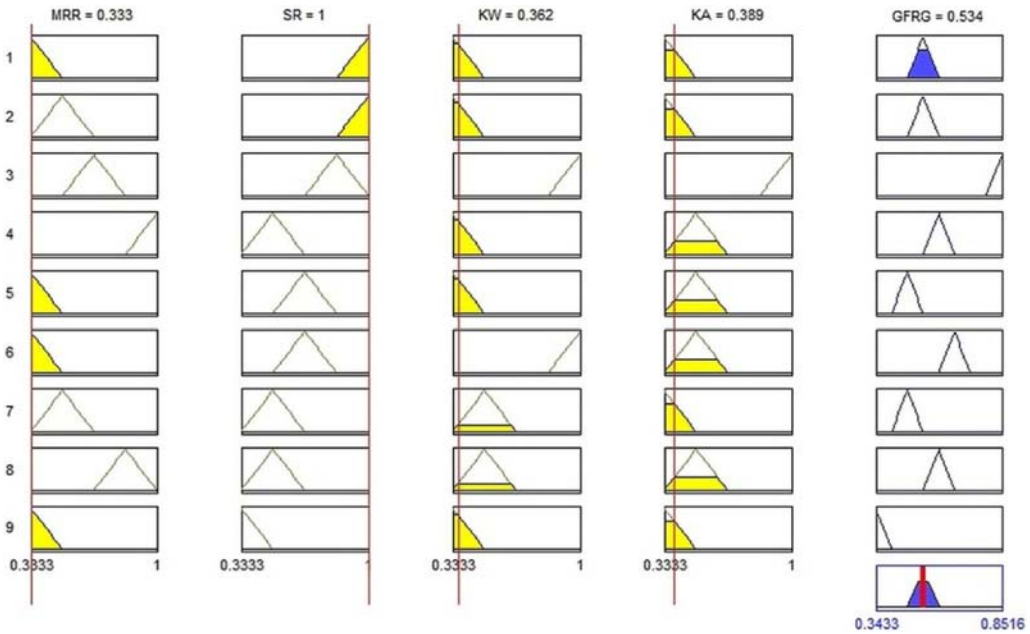

Figure 6. Rule viewer for the AWJM process.

5. Results and discussions

This section presents the application of grey-fuzzy approach in identifying the best parametric mix for the AWJM process during machining on GFRP composites. The ANOVA is performed to identify the contribution of each of the process parameters responsible for determining the GFRG values. A regression equation is also established correlating the input parameters with the calculated GFRG values and the surface plots are accordingly developed. Moreover, the interaction plots are presented illustrating the effects of the AWJM process parameters on the responses.

The experimental data, as presented in table 3, is now utilized to derive the respective GRC and GRG values. Depending on the type of quality characteristic considered and employing Eq. (3) or (4), the experimental values are pre-processed to bring them within a normalized range from 0 to 1. Based on these normalized data and applying Eqs. (5)–(6), the GRC and GRG values are then computed for all the experimental trials, as presented in table 4. The trial number 3 with the maximum GRG value is identified to be the best experiment. However, to improve the superiority of the derived solution, and reduce the uncertainty and vagueness in the experimental observations, fuzzy logic approach is consequently employed.

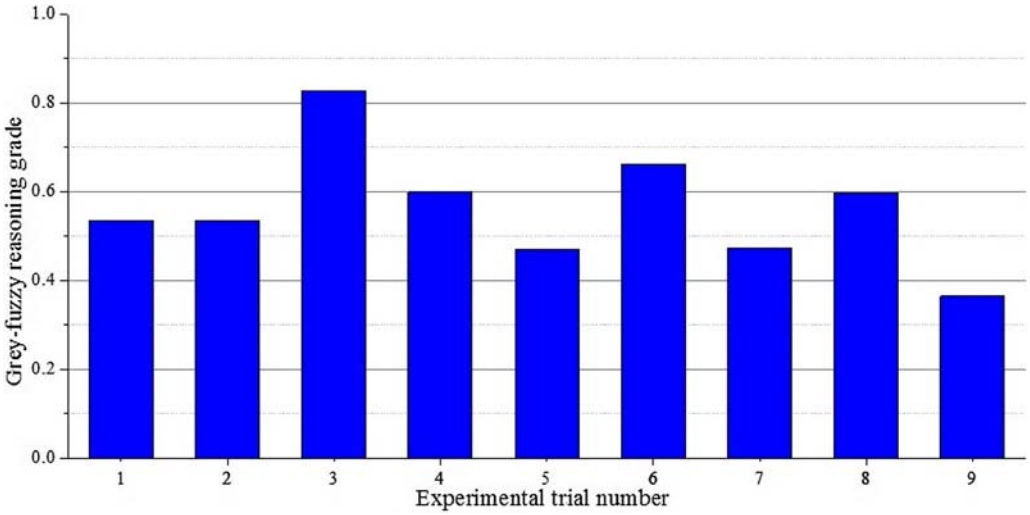

Figure 7. GFRG values for the experimental runs.

Table 5. Response table for the calculated GFRG values.

	Level				
Process parameter	1	2	3	Max–Min	Rank
Water jet pressure	**0.6313**	0.5763	0.4770	0.1543	2
Standoff distance	0.5340	0.5337	**0.6170**	0.0833	4
Abrasive mass flow rate	**0.5973**	0.4987	0.5887	0.0987	3
Traverse speed	0.4560	0.5550	**0.6737**	0.2177	1

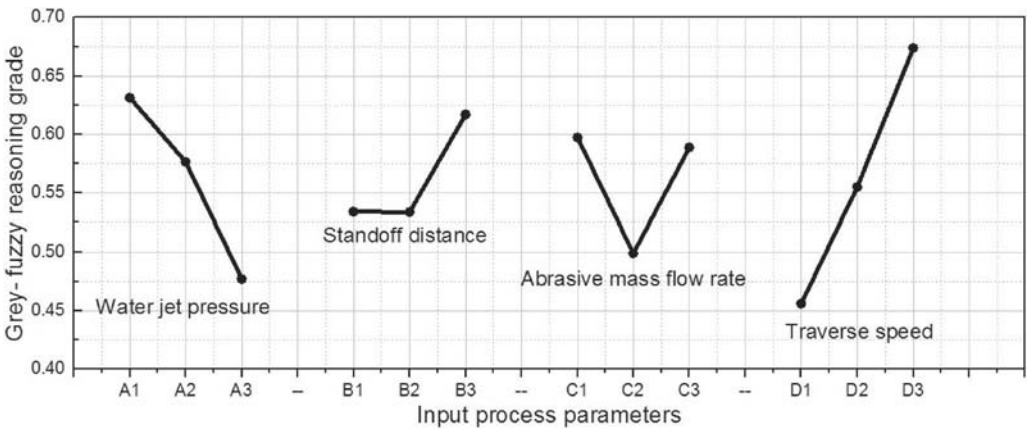

Figure 8. Response graph for calculated GFRG values.

For grey-fuzzy method-based analysis, the output GFRG values are generated with the fuzzy tool box of MATLAB (2014a). The GRC values for the four responses (MRR, SR, KW and KA) are treated as the inputs to the fuzzy system, while the only output is GFRG. Thus, the considered multi-objective problem can be structured as a four-input-one-output fuzzy system, as illustrated in figure 3. A triangular membership function with five fuzzy subsets as VL (very low), L (low), M (medium), H (high) and VH (very high) is considered here for the input GRC values with minimum

Table 6. ANOVA results for GFRG values.

Process parameter	DoF	Adj SS	Adj MS	*F*-value	*p*-value	% contribution
Water jet pressure	1	0.035728	0.035728	6.36	0.065	25.57
Standoff distance	1	0.010334	0.010334	1.84	0.247	7.40
Abrasive mass flow rate	1	0.013000	0.000113	0.02	0.894	9.30
Traverse speed	1	0.071068	0.071068	12.65	0.024	50.87
Error	4	0.009586	0.005618			6.86
Total	8	0.139716				

and maximum values as 0.3333 and 1 respectively. Another triangular membership function consisting of nine fuzzy subsets as EL (extremely low), VL (very low), L (low), ML (moderately low), M (moderate), MH (moderately high), H (high), VH (very high) and EH (extremely high) is selected for the output GFRG value having a range between 0.3433 and 0.8516. These input membership function and output membership function are respectively represented in figure 4 and figure 5. Now, based on the nine sets of experimental trials, nine rules are developed representing the associationships among the input GRC and output GFRG value. An example of such a rule is exhibited as below:

If (MRR is VL) and (SR is VH) and (KW is VL) and (KA is VL), then (GFRG is ML).

The graphical representation of these rules involved in the grey-fuzzy system, as derived from MATLAB tool box, is provided in figure 6. The rows in this figure represent the fuzzy rules established based on the nine sets of experiments, whereas, the first four columns indicate the input GRC values for the four responses and the last column shows the output GFRG value in the fuzzy system. The location of each triangle in this figure signifies the fuzzy subset associated with the fuzzy rule and the corresponding height of the colored area for each triangle denotes the fuzzy value pertaining to the membership function for a fuzzy set. It can be noticed from figure 6 that when the input GRC values for MRR, SR, KW and KA are 0.333, 1, 0.362 and 0.389 respectively, the subsequent value of GFRG is obtained as 0.534 for the first experimental run. Similarly, for all the nine experiments, the GFRG values are determined, as provided in figure 7. It can be observed from this figure that experiment number 3 with the maximum GFRG value of 0.826 comes out as the most preferred parametric setting for the AWJM process leading to concurrent optimization of the responses.

Table 5 presents the response table for the GFRG values, while taking the average of the estimated GFRG values at the operating levels of the corresponding process parameters. The maximum GFRG values at the relevant operating levels of the considered process parameters are highlighted in bold face. Figure 8 represents the response graph developed from this table. It can now be observed that to run the AWJM process at the optimal machining condition, the input parameters must be set at water jet pressure = 165 MPa, stand-off distance = 3 mm, abrasive mass flow rate = 200 g/min and traverse speed = 50 mm/min, symbolically denoted as $A_1B_3C_1D_3$. In table 4, the max–min column indicates traverse speed as the most influential AWJM control parameter which can also be verified by its steep slope in figure 8.

Table 6 presents the ANOVA results based on the calculated GFRG values. A *p*-value less than or equal to 0.05 ($p \leq 0.05$) identifies a factor as statistically significant. It can be witnessed that traverse speed is the statistically significant control parameter having a contribution of 50.87% in determination of GFRG values, followed by water jet pressure. A polynomial regression equation is also developed representing the relationships of different AWJM process parameters with the estimated GFRG values. It would mainly help the process engineers in predicting the GFRG value for any combination of the process parameters. Figure 9 presents the surface plots generated based on this regression equation. These plots basically exhibit the effects of the considered AWJM process parameters on the estimated GFRG values.

$$\begin{aligned} \text{GFRG} = {} & 1.082 + 0.002149 \times \text{A} - 0.1235 \times \text{B} - 0.005632 \\ & \times \text{C} + 0.002617 \times \text{D} - 0.000009 \times \text{A}^2 + 0.04117 \\ & \times \text{B}^2 + 0.000009 \times \text{C}^2 + 0.000102 \times \text{D}^2 \end{aligned} \tag{10}$$

5.1 *Effects on MRR*

Figure 10 exhibits the influences of varying values of the considered AWJM process parameters on the measured MRR. It can be noticed from figure 10a that at lower stand-off distance, MRR initially increases as the water jet pressure increases. It is mainly due to the fact that the water jet containing abrasives stays concentrated at a point while travelling through a small distance, making impact with higher pressure and kinetic energy on the workpiece surface, accordingly increasing the rate of erosion of the material [33]. But as the stand-off distance increases, MRR decreases. An increase in the distance from the nozzle to workpiece surface causes divergence and widening of the jet before impingement, resulting in decrease in kinetic energy density and reduction in MRR, as assessed in

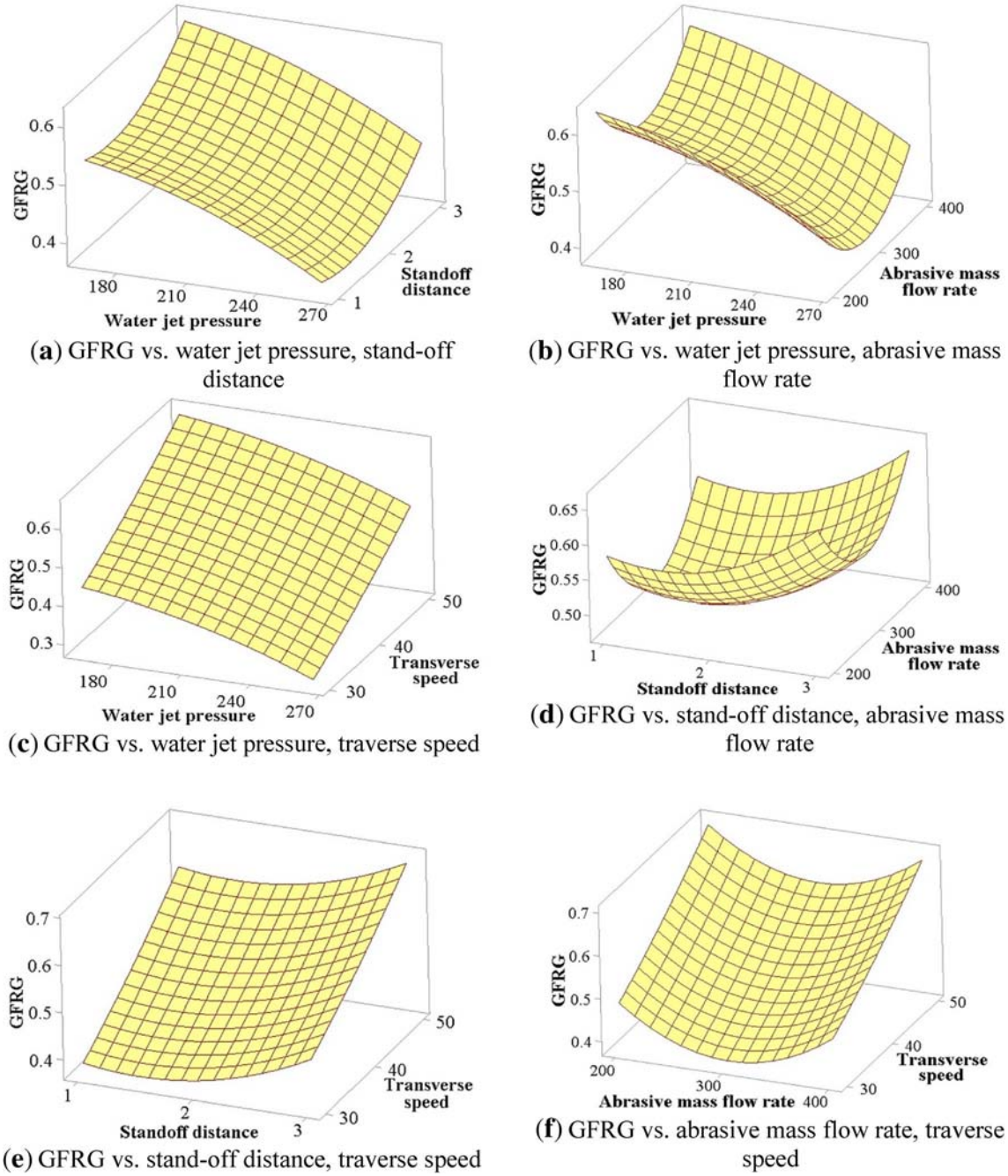

(**a**) GFRG vs. water jet pressure, stand-off distance

(**b**) GFRG vs. water jet pressure, abrasive mass flow rate

(**c**) GFRG vs. water jet pressure, traverse speed

(**d**) GFRG vs. stand-off distance, abrasive mass flow rate

(**e**) GFRG vs. stand-off distance, traverse speed

(**f**) GFRG vs. abrasive mass flow rate, traverse speed

Figure 9. Surface plots for the AWJM process.

figure 10b. An increment in mass flow rate of abrasives increases the MRR moderately, as depicted in figure 10c. The abrasives carry kinetic energy of the water and strike the workpiece surface with high impact, resulting in higher amount of abrasion. Thus increasing the density of abrasive particles further enhances the erosion rate, resulting in higher MRR. However, after a certain value, further rise in the mass flow rate of abrasive particles causes decrement in MRR due to higher inter-collisions between them. More is the abrasive mass flow rate, more would be the inter-collision, resulting in decrease in kinetic energy and resultant MRR. Figure 10d shows that a rise in the value of traverse speed rapidly increases MRR as it is directly proportional to MRR.

5.2 *Effects on SR*

The effects of the considered AWJM process parameters on the obtained SR values are presented in figure 11. Higher

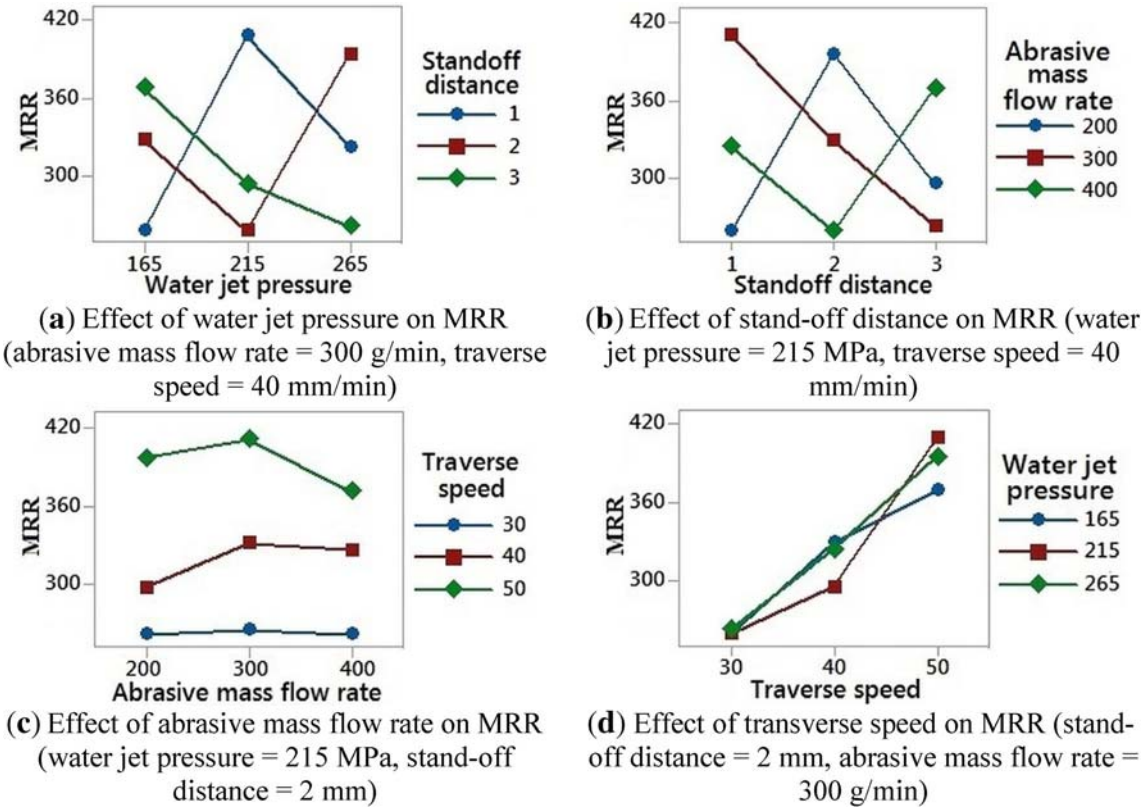

(a) Effect of water jet pressure on MRR (abrasive mass flow rate = 300 g/min, traverse speed = 40 mm/min)

(b) Effect of stand-off distance on MRR (water jet pressure = 215 MPa, traverse speed = 40 mm/min)

(c) Effect of abrasive mass flow rate on MRR (water jet pressure = 215 MPa, stand-off distance = 2 mm)

(d) Effect of transverse speed on MRR (stand-off distance = 2 mm, abrasive mass flow rate = 300 g/min)

Figure 10. Effects on MRR.

water jet pressure results in increased kinetic energy of the abrasive particles, thus reducing the severe jet deflection while minimizing the waviness pattern on the machined components [27, 30]. It enhances the capacity of the jet to efficiently remove material producing better cut surface, as illustrated in figure 11a. Similarly, as observed in figure 11b, it is appropriate to have a lower stand-off distance that further causes increment in kinetic energy. Moreover, higher stand-off distance results in widening of the jet diameter before impingement that may get affected by the external drag from the machining environment. Increment in abrasive mass flow rate increases MRR, which can through cut the composite materials more easily producing better surface finish, as noticed in figure 11c [31]. However after a certain limit, further increase in abrasive mass flow rate increases the SR due to inter-collisions of the abrasive particles, thereby reducing the kinetic energy. An increase in traverse speed causes an increment in SR, as shown in figure 11d. Higher traverse speed is responsible for less overlapping of the machining actions as well as fewer number of abrasive particles getting impacted on the surface of workpiece while increasing the SR value.

5.3 *Effects on KW*

Figure 12 demonstrates the effects of varying AWJM process parameters on the estimated KW. As revealed from figure 12a, with lower stand-off distance, the KW decreases with increase in the water jet pressure. It is due to the fact that the abrasive water jet stays concentrated throughout the cut resulting in decrease in kerf [29]. On the other hand, with an increase in stand-off distance, the jet gets widened, thereby forming larger KW, as shown in figure 12b. An increment in abrasive mass flow rate initially causes wider KW, as higher amount of abrasive particles enhances the cutting capability of the jet that generally cuts the workpiece material by abrasive impingement, resulting in increased KW, as illustrated in figure 12c. However, after a certain flow rate, further increment in the amount of abrasive particles causes the KW to decrease. Larger amount of abrasive particles results in higher jet penetration into the target material, resulting in a smooth through cut with reduced KW. Figure 12(d) reveals that increase in traverse speed reduces the KW as less quantity of abrasive particles impinges on the surface of the workpiece causing less overlapping of the machining actions while reducing the amount of material erosion and KW.

5.4 *Effects on KA*

The KA is an important machining characteristic being influenced by the collision and kinetic energy of the jet of water containing abrasive particles. Figure 13 shows how

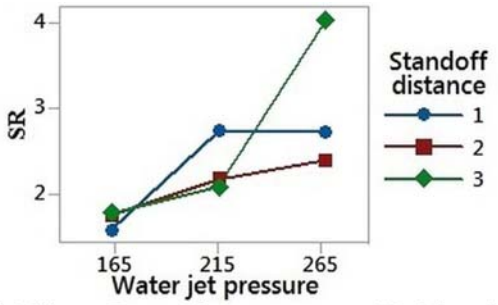

(**a**) Effect of water jet pressure on SR (abrasive mass flow rate = 300 g/min, traverse speed = 40 mm/min)

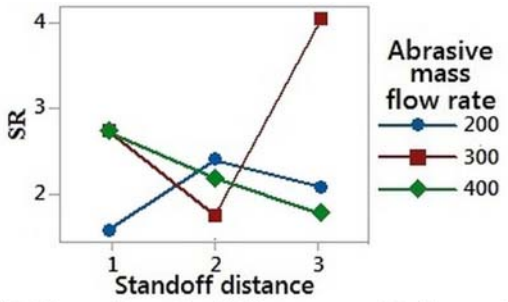

(**b**) Effect of stand-off distance on SR (water jet pressure = 215 MPa, traverse speed = 40 mm/min)

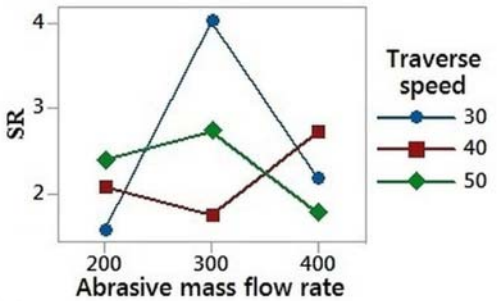

(**c**) Effect of abrasive mass flow rate on SR (water jet pressure = 215 MPa, stand-off distance = 2 mm)

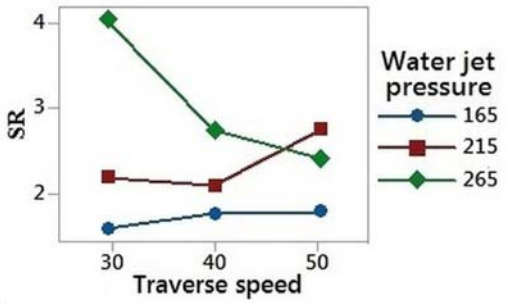

(**d**) Effect of transverse speed on SR (stand-off distance = 2 mm, abrasive mass flow rate = 300 g/min)

Figure 11. Effects on SR.

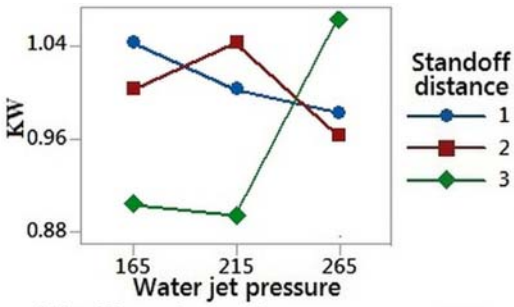

(**a**) Effect of water jet pressure on KW (abrasive mass flow rate = 300 g/min, traverse speed = 40 mm/min)

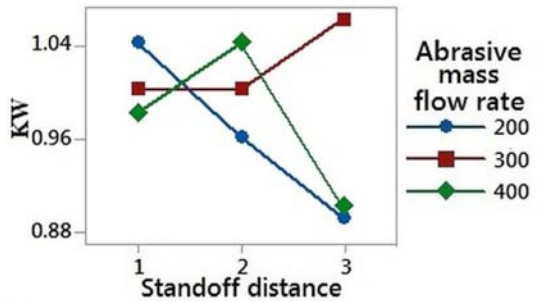

(**b**) Effect of stand-off distance on KW (water jet pressure = 215 MPa, tranerse speed = 40 mm/min)

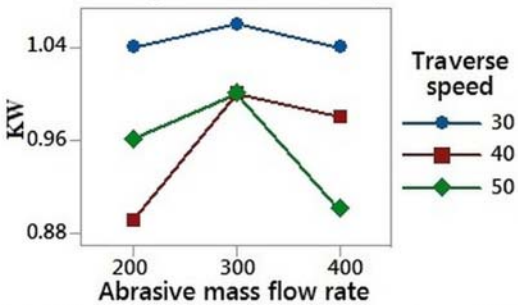

(**c**) Effect of abrasive mass flow rate on KW (water jet pressure = 215 MPa, stand-off distance = 2 mm)

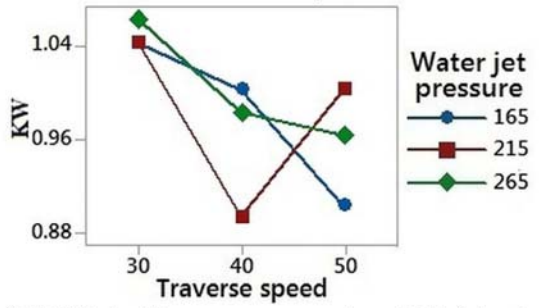

(**d**) Effect of transverse speed on KW (stand-off distance = 2 mm, abrasive mass flow rate = 300 g/min)

Figure 12. Effects on KW.

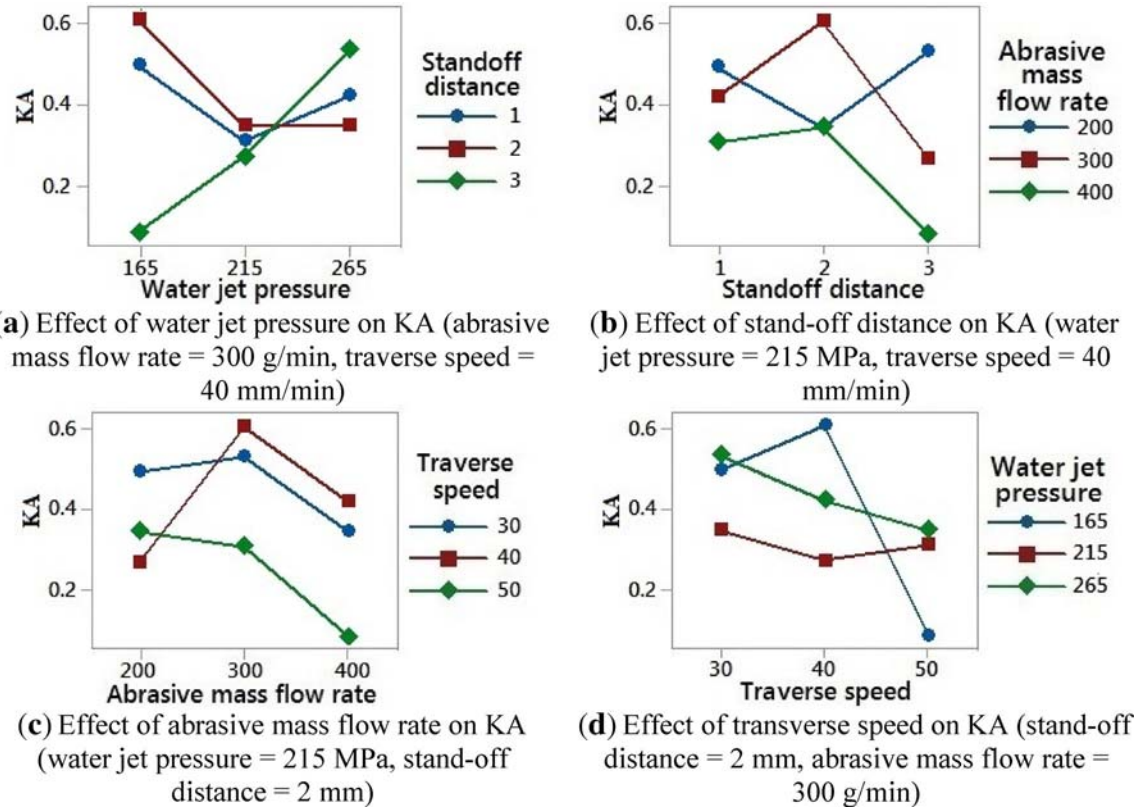

(**a**) Effect of water jet pressure on KA (abrasive mass flow rate = 300 g/min, traverse speed = 40 mm/min)

(**b**) Effect of stand-off distance on KA (water jet pressure = 215 MPa, traverse speed = 40 mm/min)

(**c**) Effect of abrasive mass flow rate on KA (water jet pressure = 215 MPa, stand-off distance = 2 mm)

(**d**) Effect of transverse speed on KA (stand-off distance = 2 mm, abrasive mass flow rate = 300 g/min)

Figure 13. Effects on KA.

Table 7. Comparison of response values.

Response	Initial parametric combination	Optimal parametric combination		
		A = 165 MPa, B = 3 mm, C = 200 g/min and D = 50 mm/min		
	A = 165 MPa, B = 1 mm, C = 200 g/min and D = 30 mm/min	Predicted	Experimental	% improvement
MRR (mm^3/min)	252		397.4	57.7
SR (μm)	1.53		1.49	2.61
KW (mm)	1.05		0.89	20.24
KA (degree)	0.5381		0.1251	76.75
GFRG	0.533	0.8352	0.831	55.91

KA changes with variations in different AWJM process parameters. The KA can be reduced with arise in jet pressure, as noticed in figure 13a. Higher value of water jet pressure generates higher kinetic energy that helps in clear through cut on the workpiece material while reducing the deviation of top kerf from bottom kerf [27, 30]. However, increasing the stand-off distance causes the jet to expand, thereby reducing the kinetic energy of the water jet before impingement. It generally results in lower depth penetration removing more material from the top surface than the bottom, accordingly increasing KA, as observed in figure 13b. Higher mass flow rate of abrasives involves in large amount of abrasive particles in the cutting process. The jet containing a high concentration of abrasive particles would have higher kinetic energy capable of penetrating through the workpiece more easily. With increase in the penetration capability, the top and bottom KWs tend to be equal, thereby reducing the KA, as noticed in figure 13c. In figure 13d, the KA tends to decrease as a result of involvement of fewer abrasive particles impinging on the

surface of workpiece, hence reducing the amount of overcut on the top surface resulting in lower KA. However, with lower water jet pressure, KA deteriorates with higher traverse speed [31]. It may be due to the fact that the quantity of abrasive particles penetrating the surface gets reduced, causing reduction in bottom kerf resulting in increased KA.

5.5 *Confirmation test*

To validate the competency of the grey-fuzzy method-based approach in determining the best parametric combination for the considered AWJM process, the predicted GFRG ($GFRG_P$) value at this combination is estimated based on Eq. (11).

$$GFRG_p = GFRG_m + \sum_{i=1}^{n} (\overline{GFRG_i} - GFRG_m) \quad (11)$$

where $GFRG_m$ is the mean of GFRG values obtained for all the experimental trial runs, n is the number of process parameters and $\overline{GFRG_i}$ is the mean GFRG value with respect to the optimal i^{th} level of the considered process parameters. It can be revealed from table 7 that the predicted GFRG value is better than that as determined at the initial machining condition.

The derived optimal parametric mix is now subjected to a confirmatory test run. Table 7 presents a comparison of the measured responses at the initial and optimal parametric settings. From this table, it can be confirmed that a parametric combination of water jet pressure = 165 MPa, stand-off distance = 3 mm, abrasive mass flow rate = 200 g/min and traverse speed = 50 mm/min causes improvements in MRR, SR, KW and KA values by 57.7%, 2.61%, 20.24% and 76.75% respectively, with an overall increment in the GFRG value by 55.91%.

6. Conclusions

This paper presents the parametric analysis of an AWJM process while machining GFRG composites with water jet pressure, stand-off distance, abrasive mass flow rate and traverse speed as the input parameters, and MRR, SR, KW and KA as the responses. Grey-fuzzy logic approach is applied for finding out the best mix of those process parameters. The conclusions of the above analysis are as follows:

(a) To achieve the most favorable response values, the corresponding AWJM process parameters must be set at water jet pressure = 165 MPa, stand-off distance = 3 mm, abrasive mass flow rate = 200 g/min and traverse speed = 50 mm/min.
(b) The ANOVA results identify traverse speed as the most influential process parameter with a contribution of 50.87% in determining the GFRG values, followed by water jet pressure having a contribution of 25.57%.
(c) Confirmatory experiment reveals that at the derived optimal parametric mix, MRR, SR, KW and KA can be improved by 57.7%, 2.61%, 20.24% and 76.75% respectively.
(d) At this combination, the GFRG value is also improved by 55.91% against that as obtained at the initial machining condition.

The application of grey system requires less information to analyze the behavior of an unknown process while providing an unbiased and consistent estimation. As few data are known for the corresponding grey model development, there is always a possibility that it may not completely represent the system dynamics. Hence, to further improve the capability of grey system, fuzzy logic is integrated with it. On the other hand, applications of other evolutionary techniques often lead to determination of those optimal parametric mixes which may not be feasible to fix in an AWJM set-up. The optimization performance of those algorithms is also seriously affected by the proper choice of their different tuning parameters.

Due to the ability of AWJM process to machine all types of thin and non-corrosive difficult-to-cut materials, it has found many industrial applications, like manufacturing, coal mining, civil and construction, oil and gas, electronics, food processing, automotive, aerospace, etc. Thus, it can be concluded that the application of grey-fuzzy method-based approach, with a strong mathematical background, can help the concerned process engineers in effectively deriving the optimal parametric mix for the considered AWJM process while exploring its fullest cutting potential.

References

[1] El-Hofy H 2005 *Advanced Machining Processes: Nontraditional and Hybrid Machining Processes*. McGraw-Hill, New York
[2] Badgujar P P and Rath M G 2014 Abrasive waterjet machining – A state of art. *IOSR J. Mech. Civ. Eng.* 11: 59–64
[3] Jain V K 1980 *Advanced Machining Processes*. Allied Publishers Private Limited, India
[4] Benedict G 1987 *Nontraditional Manufacturing Processes*. Marcel Dekker, Inc., New York
[5] Sharma V, Chattopadhyaya S and Hloch S 2011 Multi response optimization of process parameters based on Taguchi-fuzzy model for coal cutting by water jet technology. *Int. J. Adv. Manuf. Technol.* 56: 1019–1025
[6] Hutyrová Z, Ščučka J, Hloch S, Hlaváček P and Zeleňák M 2016 Turning of wood plastic composites by water jet and abrasive water jet. *Int. J. Adv. Manuf. Technol.* 84: 1615–1623
[7] Nag A, Ščučka J, Hlavacek P, Klichová D, Srivastava A K, Hloch S, Dixit A R, Foldyna J and Zelenak M 2018. Hybrid aluminium matrix composite AWJ turning using

olivine and Barton garnet. *Int. J. Adv. Manuf. Technol.* 94: 2293–2300

[8] Srivastava A K, Nag A, Dixit A R, Tiwari S, Scucka J, Zelenak M, Hloch S and Hlavacek P 2017 Surface integrity in tangential turning of hybrid MMC A359/B_4C/Al_2O_3 by abrasive waterjet. *J. Manuf. Process.* 28: 11–20

[9] Jegaraj J J R and Babu N R 2007 A soft computing approach for controlling the quality of cut with abrasive waterjet cutting system experiencing orifice and focusing tube wear. *J. Mater. Process. Technol.* 185(1–3): 217–227

[10] Azmir M A and Ahsan A K 2008 Investigation on glass/epoxy composite surfaces machined by abrasive water jet machining. *J. Mater. Process. Technol.* 198(1–3): 122–128

[11] Srinivasu D S and Babu N R 2008 A neuro-genetic approach for selection of process parameters in abrasive waterjet cutting considering variation in diameter of focusing nozzle. *Appl. Soft Comput.* 8(1): 809–819

[12] Siddiqui T U, Shukla M and Tambe P B 2008 Optimisation of surface finish in abrasive water jet cutting of Kevlar composites using hybrid Taguchi and response surface method. *Int. J. Mach. Mach. Mater.* 3(3–4): 382–402

[13] Zain A M, Haron H and Sharif S 2011 Estimation of the minimum machining performance in the abrasive waterjet machining using integrated ANN-SA. *Expert Syst. Appl.* 38(7): 8316–8326

[14] Zain A M, Haron H and Sharif S 2011 Genetic algorithm and simulated annealing to estimate optimal process parameters of the abrasive waterjet machining. *Eng. Comput.* 27(3): 251–259

[15] Pawar P J and Rao R V 2013 Parameter optimization of machining processes using teaching-learning-based optimization algorithm. *Int. J. Adv. Manuf. Technol.* 67(5–8): 995–1006

[16] Kartal F, Çetin M H, Gökkaya H and Yerlikaya Z 2014 Optimization of abrasive water jet turning parameters for machining of low density polyethylene material based on experimental design method. *Int. Polym. Process.* 29(4): 535–544

[17] Liu D, Huang C, Wang J, Zhu H, Yao P and Liu Z 2014 Modeling and optimization of operating parameters for abrasive waterjet turning alumina ceramics using response surface methodology combined with Box-Behnken design. *Ceram. Int.* 40(6): 7899–7908

[18] Mellal M A and Williams E J 2016 Parameter optimization of advanced machining processes using cuckoo optimization algorithm and hoopoe heuristic. *J. Intell. Manuf.* 27(5): 927–942

[19] Aich U, Banerjee S, Bandyopadhyay A and Das P K 2014 Multi-objective optimisation of abrasive water jet machining responses by simulated annealing and particle swarm. *Int. J. Mech. Manuf. Syst.* 7(1): 38–59

[20] Munuswamy N B and Krishnan M N 2014 Multiresponse analysis in abrasive waterjet machining process on AA 6351. *Int. J. Manuf. Mater. Mech. Eng.* 4(4): 38–48

[21] NareshBabu M and Muthukrishnan N 2014 Investigation on surface roughness in abrasive water-jet machining by the response surface method. *Mater. Manuf. Process.* 29(11–12): 1422–1428

[22] Singh D and Chaturvedi V 2014 Investigation of optimal processing condition for abrasive water jet machining for stainless steel AISI 304 using grey relational analysis coupled with S/N ratio. *Appl. Mech. Mater.* 592: 438–443

[23] Yuvaraj N and Pradeep Kumar M 2015 Multiresponse optimization of abrasive water jet cutting process parameters using TOPSIS approach. *Mater. Manuf. Process.* 30(7): 882–889

[24] Chaturvedi V and Singh D 2015 Multi response optimization of process parameters of abrasive water jet machining for stainless steel AISI 304 using VIKOR approach coupled with signal to noise ratio methodology. *J. Adv. Manuf. Syst.* 14(2): 107–121

[25] Ghosh D, Doloi B and Das P K 2015 Parametric analysis and optimisation on abrasive water jet cutting of silicon nitride ceramics. *Int. J. Precis. Technol.* 5(3–4): 294–311

[26] Ibraheem H M A, Iqbal A and Hashemipour M 2015 Numerical optimization of hole making in GFRP composite using abrasive water jet machining process. *J. Chin. Inst. Eng.* 38(1): 66–76

[27] Santhanakumar M, Adalarasan R and Rajmohan M 2015 Experimental modelling and analysis in abrasive waterjet cutting of ceramic tiles using grey-based response surface methodology. *Arab. J. Sci. Eng.* 40(11): 3299–3311

[28] Nair A and Kumanan S 2017 Multi-performance optimization of abrasive water jet machining of Inconel 617 using WPCA. *Mater. Manuf. Process.* 32(6): 693–699

[29] Shukla R and Singh D 2017 Experimentation investigation of abrasive water jet machining parameters using Taguchi and evolutionary optimization techniques. *Swarm Evol. Comput.* 32: 167–183

[30] Kumar A, Singh H and Kumar V 2018 Study the parametric effect of abrasive water jet machining on surface roughness of Inconel 718 using RSM-BBD techniques. *Mater. Manuf. Process.* 33(13): 1483–1490

[31] Babu M N and Muthukrishnan N 2018 Exploration on kerf-angle and surface roughness in abrasive waterjet machining using response surface method. *J. Inst. Eng. Series C* 99(6): 645–656

[32] Chakraborty S and Mitra A 2018 Parametric optimization of abrasive water-jet machining processes using grey wolf optimizer. *Mater. Manuf. Process.* 33(13): 1471–1482

[33] Kumar K R, Sreebalaji V S and Pridhar T 2018 Characterization and optimization of abrasive water jet machining parameters of aluminium/tungsten carbide composites. *Measurement* 117: 57–66

[34] Deng J 1989 Introduction to grey system theory. *J. Grey Syst.* 1(1): 1–24

[35] Zadeh L 1965 Fuzzy sets. *Inf. Control* 8(3): 338–353

[36] Chakraborty S, Das P P and Kumar V 2018 Application of grey-fuzzy logic technique for parametric optimization of non-traditional machining processes. *Grey Syst. Theory and Appl.* 8(1): 46–68

[37] Liu N M, Horng J T and Chiang K T 2009 The method of grey-fuzzy logic for optimizing multi-response problems during the manufacturing process: A case study of the light guide plate printing process. *Int. J. Adv. Manuf. Technol.* 41(1): 200–210

[38] Pandey R K and Panda S S 2014 Optimization of bone drilling parameters using grey-based fuzzy algorithm. *Measurement* 47:386–392

[39] Kumaran S T, Ko T J and Kurniawan R 2018 Grey fuzzy optimization of ultrasonic-assisted EDM process parameters for deburring CFRP composites. *Measurement* 123: 203–212

[40] Das P P, Diyaley S, Chakraborty S and Ghadai R K 2019 Multi-objective optimization of wire electro discharge machining (WEDM) process parameters using grey-fuzzy approach. *Period. Polytech. Mech. Eng.* 63(1): 16–25

[41] Kumar R, Hynes N R J, Pruncu C I and Sujana J A J 2019 Multi-objective optimization of green technology thermal drilling process using grey-fuzzy logic method. *J. Clean. Prod.* 236: 1–14